Cell Reports
Article

A Hybrid Mechanism of Action for BCL6 in B Cells Defined by Formation of Functionally Distinct Complexes at Enhancers and Promoters

Katerina Hatzi,[1] Yanwen Jiang,[1,2] Chuanxin Huang,[1] Francine Garrett-Bakelman,[1] Micah D. Gearhart,[3] Eugenia G. Giannopoulou,[2] Paul Zumbo,[2] Kevin Kirouac,[4] Srividya Bhaskara,[5] Jose M. Polo,[6] Matthias Kormaksson,[7] Alexander D. MacKerell, Jr.,[8] Fengtian Xue,[8] Christopher E. Mason,[2] Scott W. Hiebert,[5] Gilbert G. Prive,[4] Leandro Cerchietti,[1] Vivian J. Bardwell,[3] Olivier Elemento,[2,*] and Ari Melnick[1,*]

[1]Division of Hematology and Medical Oncology, Weill Cornell Medical College, Cornell University, New York, NY, 10065, USA
[2]Institute for Computational Biomedicine, Weill Cornell Medical College, Cornell University, New York, NY 10065, USA
[3]Developmental Biology Center, Masonic Cancer Center, and Department of Genetics, Cell Biology, and Development, University of Minnesota, Minneapolis, MN 55455, USA
[4]Division of Cancer Genomics and Proteomics, Ontario Cancer Institute, 101 College Street, Toronto, ON M5G 1L7, Canada
[5]Department of Biochemistry, Vanderbilt University, Nashville, TN 37232, USA
[6]Australian Regenerative Medicine Institute and Department of Anatomy and Development Biology, Monash University, Victoria 3800, Australia
[7]Division of Biostatistics and Epidemiology, Weill Cornell Medical College, Cornell University, New York, NY 10065, USA
[8]Department of Pharmaceutical Sciences, School of Pharmacy, University of Maryland, 20 Penn Street, Baltimore, MD 21201, USA
*Correspondence: ole2001@med.cornell.edu (O.E.), amm2014@med.cornell.edu (A.M.)
http://dx.doi.org/10.1016/j.celrep.2013.06.016

SUMMARY

The BCL6 transcriptional repressor is required for the development of germinal center (GC) B cells and diffuse large B cell lymphomas (DLBCLs). Although BCL6 can recruit multiple corepressors, its transcriptional repression mechanism of action in normal and malignant B cells is unknown. We find that in B cells, BCL6 mostly functions through two independent mechanisms that are collectively essential to GC formation and DLBCL, both mediated through its N-terminal BTB domain. These are (1) the formation of a unique ternary BCOR-SMRT complex at promoters, with each corepressor binding to symmetrical sites on BCL6 homodimers linked to specific epigenetic chromatin features, and (2) the "toggling" of active enhancers to a poised but not erased conformation through SMRT-dependent H3K27 deacetylation, which is mediated by HDAC3 and opposed by p300 histone acetyltransferase. Dynamic toggling of enhancers provides a basis for B cells to undergo rapid transcriptional and phenotypic changes in response to signaling or environmental cues.

INTRODUCTION

The BCL6 transcriptional repressor is required for formation of germinal centers (GCs) during T cell-dependent immune responses (Ci et al., 2008). BCL6 also plays a critical role in initiation and maintenance of B cell lymphomas derived from GC B cells such as diffuse large B cell lymphomas (DLBCLs) (Ci et al., 2008). Defining the mechanism of action of BCL6 is of crucial importance to understanding the biology of B cells and the molecular pathogenesis of BCL6-dependent lymphoid neoplasms. BCL6 is a member of the BTB-POZ C2H2 zinc finger family of transcription factors (Stogios et al., 2005). The BCL6 BTB domain has autonomous repressor activity and folds as an obligate homodimer (Ahmad et al., 2003). The dimer interface forms two extended grooves that serve as docking sites for three corepressors: SMRT, NCOR, and BCOR (Ahmad et al., 2003; Ghetu et al., 2008). SMRT and NCOR are highly conserved and bind to the BCL6 BTB groove with an identical peptide sequence. They form a complex with TBL1, TBLR1, GPS2, and HDAC3 and allosterically enhance HDAC3-mediated H3K9 acetylation (Karagianni and Wong, 2007). BCOR shares no sequence or structure similarity with SMRT/NCOR and binds to BCL6 using a completely different peptide sequence (Ahmad et al., 2003; Ghetu et al., 2008). BCOR forms a Polycomb repressor complex 1 (PRC1)-like complex with PCGF1, KDM2B, RING1, SKP1, RYBP, and RNF2 (Farcas et al., 2012; Gao et al., 2012; Gearhart et al., 2006; Sánchez et al., 2007). BTB point mutations that disrupt corepressor recruitment inactivate BTB domain repressor function (Ahmad et al., 2003; Ghetu et al., 2008). A similar effect can be achieved using specific BCL6 BTB groove binding peptides or small molecules (Cerchietti et al., 2009, 2010a; Polo et al., 2004). The BTB domain corepressor interaction is an important mediator of BCL6 actions and a potential therapeutic target (Ci et al., 2008; Parekh et al., 2008), yet it is not known how these protein interactions translate into transcriptional repression and where and how different BCL6

complexes assemble in the genome. Herein, we confirm that BTB-corepressor interactions are absolutely required for survival of both malignant and normal B cells. We show that BCL6 mediates these effects through two functionally distinct mechanisms. The first involves formation of a unique ternary complex whereby BCL6 can coordinate the actions of the BCOR Polycomb-like complex with SMRT/NCOR to potently repress target genes. The second involves a mechanism for ''toggling'' active enhancers into a ''poised'' configuration through SMRT-HDAC3-dependent H3K27 deacetylation. This function for HDAC3 enables BCL6-SMRT complexes to compete with p300 in switching enhancers between ''on'' and ''off'' states. Reversible enhancer toggling may be critical for dynamic modulation of the BCL6 transcriptional program during the GC reaction as well for the therapeutic effects of BCL6 inhibitors.

RESULTS

Distinct Genomic Localization Patterns of Specific BCL6-Corepressor Complexes

To evaluate the full impact of disrupting BCL6 BTB domain interactions with corepressors in DLBCL cells, we treated mice bearing human DLBCL cell line xenografts with RI-BPI, a peptidomimetic that specifically disrupts the BCL6 BTB domain interaction with SMRT, NCOR, and BCOR corepressors (Cerchietti et al., 2009; Polo et al., 2004). Low doses of RI-BPI (25 mg/kg/day) given to mice were shown to slow DLBCL tumor growth (Cerchietti et al., 2009). In the current study, we administered RI-BPI (50 mg/kg) or control peptide for 5 days to mice bearing established human DLBCL xenografts. RI-BPI caused complete regression of fully established DLBCL tumors in 100% of mice (Figure 1A). There was no microscopic evidence of residual tumor or tumor regrowth after treatment discontinuation in 60% of these mice. Hence, the BCL6 BTB domain corepressor recruitment is essential for the survival of BCL6-dependent human DLBCL cells. To dissect out the transcriptional mechanisms through which BCL6 and its corepressors mediate these essential functions, we next performed chromatin immunoprecipitation sequencing (ChIP-seq) for these proteins in DLBCL cells (OCI-Ly1). All ChIP-seq assays met ENCODE quality criteria (Table S1). Using stringent peak detection thresholds and the overlap of two highly correlated biological replicates ($r = 0.84$), we identified 14,780 BCL6 binding sites corresponding to the most highly enriched peaks (Figures S1A and S1B). Most BCL6 peaks localized to intronic (42%) and intergenic regions (31%), whereas 23% located to promoters (Figure 1B). The BCL6 DNA binding motif (Ci et al., 2009) was highly overrepresented ($p < 1 \times 10^{-8}$) and preferentially localized near the BCL6 peak summits (Figure S1C). BCL6 was enriched at well-known BCL6 targets such as *BCL6* itself (Wang et al., 2002), *PRDM1* (Shaffer et al., 2000), *TP53* (Phan and Dalla-Favera, 2004), *EP300* (Cerchietti et al., 2010b), *BCL2* (Ci et al., 2009; Saito et al., 2009), and *ATR* (Ranuncolo et al., 2007) (Figure S1D).

Our ChIP-seq analysis of BCL6 corepressors identified 4,379 SMRT, 4,302 NCOR, and 17,548 BCOR high-quality peaks (Figures S1E, S1F, and S2A). Strikingly 90% of SMRT and NCOR peaks overlapped with BCL6, suggesting that their function is mostly tied to BCL6 in DLBCL (Figures 1C and S2A). Even though NCOR and SMRT can bind to many transcription factor partners (Perissi et al., 2010), it appears that association with BCL6 is their dominant function in the B cell context. Reciprocally, only 27% of BCL6 peaks were occupied by NCOR-SMRT. BCL6-SMRT and BCL6-NCOR complexes exhibit extensive binding in intergenic and intronic regions with proportionally less promoter binding (Figure 1B). Because SMRT and NCOR were mostly colocalized and have similar biochemical functions ($r = 0.76$, Pearson; Figure S1E), we focused on SMRT for subsequent analyses. BCOR occupied 36% of BCL6 peaks and was more widely distributed to non-BCL6-containing peaks than SMRT/NCOR, suggesting that it may have BCL6-independent functions (Figure 1C). In contrast to BCL6-SMRT, BCL6-BCOR complexes were more frequently localized to promoters (Figure 1B). Consistent with previous studies (Ci et al., 2009), BCL6 corepressor peaks contain binding sites for other transcription factors, including STAT sites (which overlap with BCL6 motif; Dent et al., 1997) RUNX1 and ELK1, which might either compete or cooperate with BCL6. BCOR-BCL6 peaks were preferentially enriched in CG-rich sequences, consistent with their frequent localization in CpG islands (35%; 1,830/5,265 peaks). On the other hand, BCL6-SMRT peaks were preferentially enriched in MEF2A motifs (Figure S2B). Notably, 13% of BCL6 binding sites contain both SMRT and BCOR peaks, suggesting that BCL6 may simultaneously recruit both corepressors at certain BCL6 binding sites (Figure 1C).

We also performed ChIP-seq for BCL6, SMRT, NCOR, and BCOR in purified primary human GC B cells, from which DLBCLs arise (Figures S2C, S2D, S2G, and S2H). Seventy-eight percent of BCL6 target genes in DLBCL cells overlapped with GC B cells, and 85% of target genes with BCL6-corepressor complexes in DLBCL also contained such complexes in GC B cells, although GC B cells also have additional unique targets (Figure S2E and S2F). Most importantly, the genome-wide distribution of BCL6 and corepressors was highly similar to DLBCL cells with comparable distributions to promoters and intergenic/intronic regions and ~90% overlap of SMRT with BCL6 (Figure S2G and S2H). These results suggest that recruitment of these corepressors may be just as vital for normal GC B cells as for DLBCL cells. Confirming this hypothesis, knockin mice expressing a $BCL6^{N21KH116A}$ lateral groove mutant, which is unable to recruit SMRT, NCOR, and BCOR but is otherwise normally expressed, folded, and bound to target genes (Ahmad et al., 2003; Ghetu et al., 2008), fail to form GCs (Figure S3A) (Huang et al., 2013).

BCL6 Forms SMRT/BCOR Ternary Complexes to Potently Repress Expression

To understand the significance of BCL6 and corepressor distribution patterns relative to gene expression, we initially focused on BCL6 promoter complexes. BCL6 was bound to the promoters of 3,140 genes in DLBCL cells, 71% of which were occupied by overlapping BCL6-corepressor peaks. Overall, BCL6 binding sites at promoters could be classified into four classes: (1) BCL6 only ($n = 906$), (2) BCL6-SMRT only ($n = 92$), (3) BCL6-BCOR only ($n = 1,783$), and (4) BCL6-SMRT-BCOR ($n = 341$) (Figure S3B). At these latter sites, BCL6-SMRT-BCOR were all colocalized, suggesting that these are BCL6-dependent ternary complexes. The requirement of BCL6 to recruit BCOR

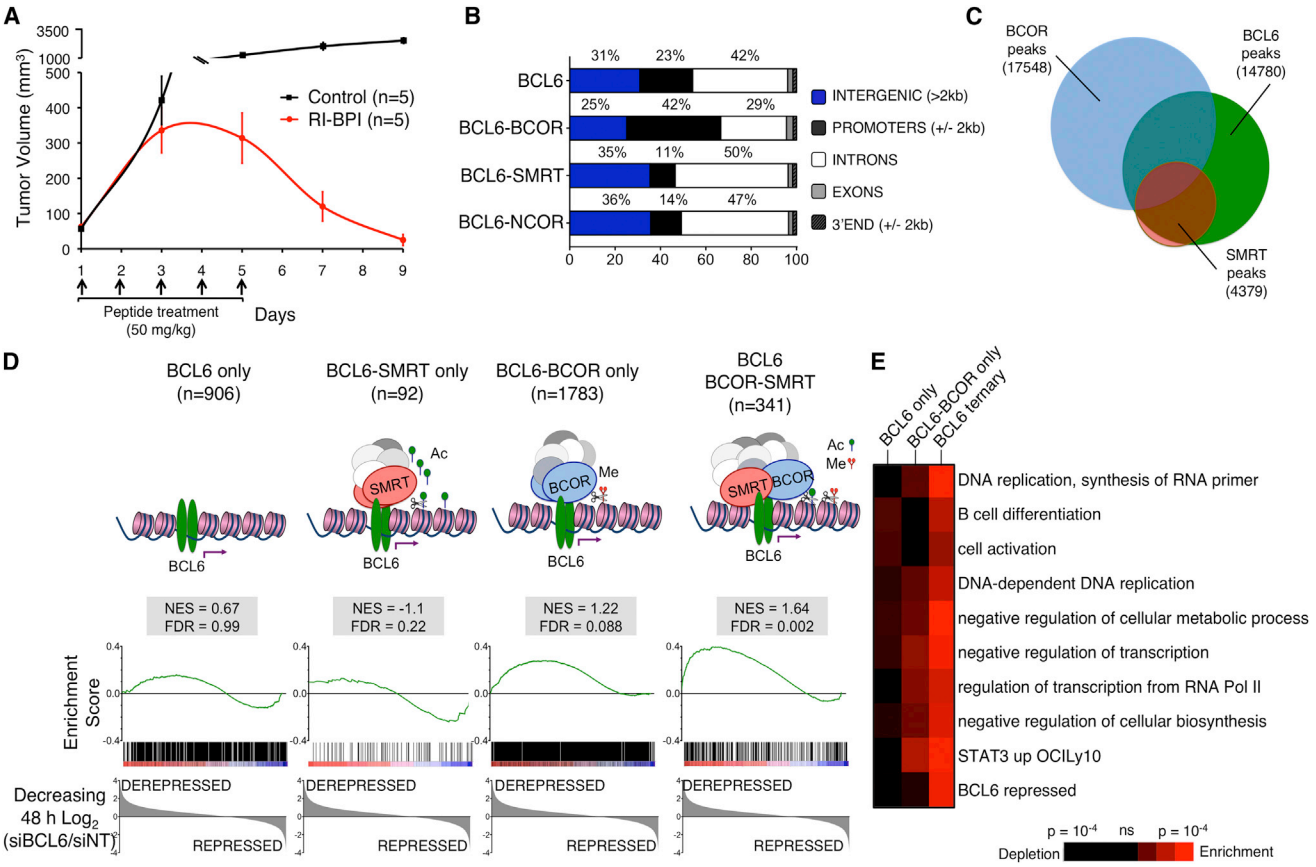

Figure 1. Genome-wide Distribution of BCL6 and Corepressors BCOR, SMRT, and NCOR in DLBCL Cells

(A) Tumor growth plot in DLBCL xenografted mice (Farage cell line) after treatment with RI-BPI versus control peptide (50 mg/kg/day for 5 consecutive days). Data are represented as mean ± SEM.

(B) Genomic distribution of BCL6 peaks and BCL6 peaks coinciding with BCOR (BCL6-BCOR), SMRT (BCL6-SMRT), and NCOR (BCL6-NCOR) peaks based on their location relative to RefSeq transcripts (hg18) in OCI-Ly1 cells.

(C) Venn diagrams representing the overlap of BCL6, BCOR, and SMRT ChIP-seq peaks in DLBCL cells.

(D) GSEA analysis integrating ChIP-seq and mRNA-seq results after BCL6 knockdown. The enrichment of promoter target genes bound by BCL6 ternary complexes (BCL6-BCOR-SMRT), BCL6-BCOR only, BCL6-SMRT only, or BCL6 only was tested based on decreasing gene all expression log ratios (48 hr; siBCL6/siNT). Weighed statistic and 5,000 sample permutations were used. NES, normalized enrichment score; FDR, false discovery rate.

(E) Pathway analysis comparing BCL6-BCOR only target genes versus BCL6-ternary target genes that were upregulated more than 1.5-fold after BCL6 knockdown.

See also Figures S1, S2, S3, S4, and S5 and Table S1.

and SMRT was confirmed by performing ChIP assays at representative promoters (*PRDM1*, *TLR4*, and *CD69*) 24 hr after BCL6 or control small interfering RNA (siRNA) transduction in DLBCL cells. Recruitment of both corepressors was reduced proportionally to BCL6 depletion (Figure S3C).

To determine the relative contribution of these different BCL6 complexes to gene expression, we performed messenger RNA sequencing (mRNA-seq) at 24 hr and 48 hr after transduction of BCL6 or control siRNA in DLBCL cells (Figures S4A and S4B). Derepression of BCL6 promoter target genes was the dominant effect after BCL6 knockdown (approximately 70% of genes upregulated). We used gene set enrichment analysis (GSEA) to determine which type of BCL6 complex (BCL6 only, BCL6-BCOR only, BCL6-SMRT only, and BCL6-SMRT-BCOR) was most strongly associated with gene derepression (Figure 1D). This analysis revealed strong enrichment of BCL6 ternary complex (BCL6-SMRT-BCOR) among derepressed genes (false discovery rate [FDR] = 0.002). BCL6-BCOR only promoters were mildly enriched in derepressed genes with only a trend toward statistical significance (FDR = 0.088). Genes bound by BCL6-SMRT only or BCL6 without corepressors were not significantly affected by BCL6 depletion (FDR = 0.22 and FDR = 0.99, respectively). Accordingly, BCL6 ternary complex genes were more significantly derepressed when compared with BCL6-only, BCL6-SMRT only, or BCL6-BCOR only complexes ($p = 0.0026$, $p = 0.0014$, and $p = 0.019$, respectively; Mann-Whitney) (Figure S4C). Similar effects were observed at both 24 and 48 hr (Figures S4D and S4E). These results were confirmed in three additional independent mRNA-seq experiments in DLBCL cells after BCL6 versus control siRNA knockdowns (Figure S5). Derepressed

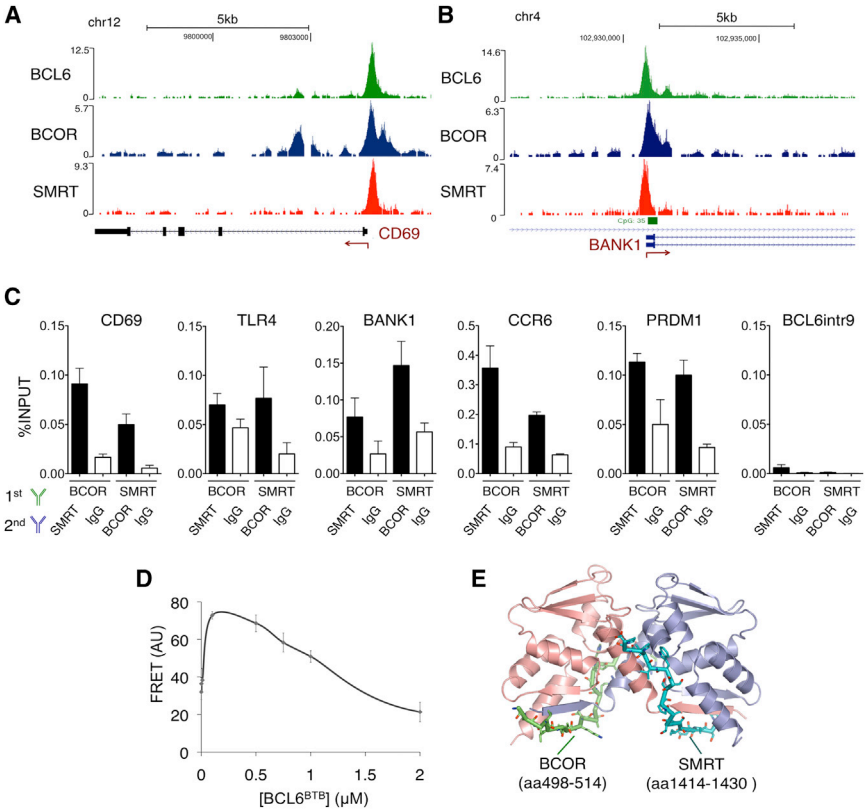

Figure 2. BCL6 Can Recruit Both BCOR and SMRT Corepressor Complexes Simultaneously through Homodimerization of its BTB Domain in Promoters

(A and B) BCL6 binding (green) at the promoters of *CD69* and *BANK1* coincides with binding of corepressors BCOR (blue) and SMRT (red), respectively. y axis values represent read densities normalized to total number of reads.

(C) ChIP-re-ChIP assay in BCL6-BCOR-SMRT promoters using BCOR and SMRT antibodies. IgG was used as a negative control. A *BCL6* intron 9 locus is shown as a negative control. The experiment was performed in duplicate using triplicate wells. The y axis represents enrichment as % input ± SEM.

(D) FRET assay for A488-BCOR and BODIPY-SMRT peptides in solution with BCL6 BTB. Fluorescence (AU) is shown as a function of increasing BCL6 BTB concentration. FRET emission is generated when both peptides bind to the BCL6 BTB dimer. Higher concentrations of BCL6 BTB dimers increase single peptide binding events decreasing FRET emission. Error bars indicate SD.

(E) Hybrid model of the BCL6 BTB dimer (each monomer in violet and pink) simulated in complex with two peptides corresponding to BCOR 498-514 (green) and SMRT 1414-1430 (cyan) used in the FRET assay.

See also Figure S6.

genes with BCL6 ternary complexes were also most significantly enriched in gene categories linked with the canonical and biologically validated BCL6 functions (Basso et al., 2004; Ci et al., 2009), including B cell differentiation, B cell activation, DNA replication, genes induced by STAT3 (Lam et al., 2008), and genes repressed by BCL6 in independent data sets (Shaffer et al., 2000) (Figure 1E). Hence, ternary promoter complexes are most strongly linked to active repression by BCL6 and to canonical BCL6 biological functions.

BCL6 forms an obligate homodimer with two symmetric lateral grooves and so could theoretically bind to BCOR and SMRT simultaneously. To determine if BCL6 forms a true ternary complex, we performed sequential ChIP (ChIP-re-ChIP) using BCOR or SMRT antibody followed by a second immunoprecipitation switching the two antibodies or using immunoglobulin G (IgG) control. We then performed quantitative PCR (qPCR) to enrich promoter binding sites with overlapping BCL6/BCOR/SMRT peaks (*CD69*, *BANK1*, *PRDM1*, *TLR4*, and *CCR6* shown in Figures 2A, 2B, and S6A). In each case, sequential immunoprecipitation enriched these loci consistent with formation of ternary BCL6-SMRT-BCOR complexes (Figure 2C). As a positive control, we performed ChIP-re-ChIP with BCL6 antibody followed by BCOR or SMRT ChIP (Figure S6B). To further confirm ternary binding, we performed fluorescence resonance energy transfer (FRET) assays in which the BCL6 BTB homodimer (Stogios et al., 2005) and fluorescent BCOR and SMRT BCL6 binding polypeptides were placed together in solution (Ahmad et al., 2003; Ghetu et al., 2008). This experiment resulted in a FRET signal, indicating that BCOR and SMRT fragments bind simultaneously to the homodimer (Figure 2D), as illustrated in Figure 2E. At higher concentrations of BCL6 BTB dimer, the majority of the peptides exist as single corepressor peptide/BCL6 BTB complexes, which produce no FRET signal (Figure 2D). Hence, the BCL6 BTB dimer is able to coordinate assembly of a multifunctional ternary corepressor complex at gene promoters including both the PRC1-like BCOR and the HDAC3-containing SMRT complex.

BCL6 Repression Is Linked to Specific Chromatin States and RNA Polymerase II Pausing

In order to understand the chromatin context within which BCL6 is functional as a repressor, we performed ChIP-seq for the H3K4me3, H3K9ac, H3K79me2, and H3K36me3 activation marks and the H3K27me3 repressive mark and enhanced reduced representation bisulfite sequencing (ERRBS) for cytosine methylation in DLBCL cells. We then used an unbiased analysis approach (multidimensional principal component analysis) to group gene promoters according to the naturally occurring binding patterns of BCL6, corepressors, histone modifications, and cytosine methylation (Figure 3A). We found that genes linked to principal component 2 (PC2) featured significantly lower transcript levels in DLBCL cells ($p < 1 \times 10^{-8}$) and, most importantly, significant derepression after BCL6 siRNA ($p < 1 \times 10^{-8}$; Figure 3B). PC2 promoters were significantly enriched for BCL6, SMRT, and BCOR as well as repression marks H3K27me3 and cytosine methylation but at the same time were markedly

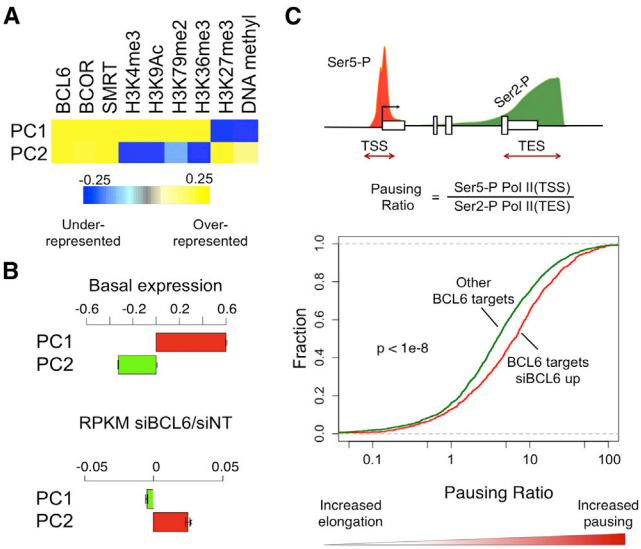

Figure 3. Potent BCL6 Repression Occurs within Repressed Chromatin States and Is Linked to RNA Pol II Pausing

(A) Graphical representation of weighted PCA analysis integrating histone mark and DNA methylation enrichment levels surrounding all TSSs. The top two PCs are shown. The color key indicates the weights of the original variables assayed by ChIP-seq and ERRBS.

(B) Correlation of genes corresponding in each PC with basal levels of gene expression and gene expression changes after BCL6 knockdown (48 hr) is indicated.

(C) Cumulative distribution of RNA Pol II pausing ratios (calculated as the fraction of normalized read density ratio of Ser5-P Pol II (paused) around the TSS (−100 to +200 bp) to the Ser2-P Pol II (elongating) density at the TES (TES +2 kb) comparing BCL6 target genes upregulated after BCL6 siRNA versus the rest of BCL6 target genes. p value is indicated.

See also Figure S7.

depleted of all four active histone marks. In contrast, PC1 captured active genes associated with binding but not repression by BCL6. Overall, the principal component analysis (PCA) analysis indicated that only promoters with ternary complexes plus a completely repressed chromatin configuration are actively repressed by BCL6. BCL6 does not appear to be functionally significant at promoters with activation marks or where BCL6 is not forming a ternary complex.

Analysis of promoter ChIP-seq profiles further indicated that BCL6 binding occurred within the nucleosome-free region (NFR) located just upstream of the transcriptional start site (TSS) as revealed by the valley of low H3K4me3 abundance (Figure S7A). SMRT and BCOR were precisely overlapped with BCL6 except that BCOR extended further downstream of the TSS, where RNA polymerase II (RNA Pol II) is localized in DLBCL cells. Indeed, ChIP-seq for paused (phosphoSer5) and elongating (phosphoSer2) RNA Pol II in DLBCL cells revealed that BCL6-repressed genes had a significantly higher paused versus elongating Pol II ratio compared to nonrepressed BCL6 targets ($p < 1 \times 10^{-8}$; Figures 3C and S7C). This was independently confirmed by analyzing the distribution of total RNA pol II by ChIP-seq in DLBCL cells ($p < 1 \times 10^{-8}$; Figure S7B). Altogether, potent BCL6 repression of promoters in B cells is linked to ternary BCL6-SMRT-BCOR corepressor complex formation within a specific chromatin context featuring loss of activating and gain of repressive marks and suppression of RNA Pol II elongation but not Pol II recruitment (Figure S7D).

BCL6-SMRT Complexes Inactivate B Cell Enhancers to Repress Proximal Gene Expression

Most BCL6-SMRT binding (85%) occurred outside of promoters, suggesting that the BCL6 mechanism may differ at these sites and is perhaps linked to enhancer regions (Figure 4A). Enhancers are characterized by the presence of H3K4me1 and absence of H3K4me3 (Heintzman et al., 2007, 2009). We therefore performed H3K4me1 ChIP-seq to map enhancer regions in DLBCL cells. The vast majority of BCL6-SMRT distal/intronic peaks were $H3K4me3^{NEG}/H3K4me1^{POS}$ (n = 2,162), suggesting that these complexes are within transcriptional enhancers (Figure 4A). We first focused on distal BCL6-SMRT enhancer binding sites (n = 818, >5 kb away from TSSs). BCL6 and SMRT peak summits were precisely colocalized at enhancers and generally restricted to a narrow region of less than 400 bp framed by two adjacent nucleosomes as indicated by H3K4me1 read density (Figure 4B). These BCL6-SMRT enhancers were significantly conserved as compared to adjacent control regions, which is suggestive of their functional relevance (Figure S8A).

We next examined whether BCL6-SMRT binding to enhancers has a *cis*-regulatory function. Since most BCL6-SMRT enhancers were located within 80 kb from the nearest transcript (Figure S8B), we identified the most proximal gene for every BCL6-SMRT distal enhancer (n = 553). Using GSEA, we found that the group of genes with BCL6-SMRT-bound enhancers were significantly enriched in genes derepressed after BCL6 knockdown (FDR = 0.005 at 24 hr and FDR = 0.03 at 48 hr; Figures 4C and S8C). In contrast, genes associated with distal enhancers bound by BCL6 without SMRT (n = 654) were not enriched among BCL6 siRNA-derepressed genes (FDR = 0.38 at 24 hr and FDR = 0.68 at 48 hr; Figures 4C and S8C). Similarly, BCL6-SMRT enhancer linked genes (but not BCL6 only) were significantly upregulated after BCL6 knockdown (BCL6-SMRT: $p < 0.0001$ at 24 hr and $p = 0.032$ at 48 hr; BCL6 only: $p = 0.07$ at 24 hr and $p = 0.49$ at 48 hr; Mann-Whitney U) compared to control genes (Figures 4D and S8D).

To further investigate whether BCL6 can repress through enhancer binding we performed reporter assays using constructs containing a BCL6-SMRT enhancer identified by our ChIP-seq, located 13 kb upstream of the *CDKN1A* promoter and containing a BCL6 consensus binding motif (Figures 4E and S8E). Addition of *CDKN1A* distal enhancer induced 3-fold repression of *CDKN1A* promoter when transfected in DLBCL cells, and this repressor activity was markedly attenuated by BCL6 knockdown ($p < 0.0001$, Mann-Whitney U; Figure 4F). Enhancer with mutated BCL6 binding site was unable to repress luciferase activity and instead enhanced *CDKN1A* promoter activity (Figure 4F). BCL6 knockdown did not induce higher expression from the mutant reporter. In 293T cells, the *CDKN1A* distal enhancer acted as an inducer of transcriptional activity (Figure S8F). However, transfection of BCL6 (but not control plasmid) suppressed this *CDKN1A* enhancer activity. Collectively, these data support the notion that BCL6 can repress enhancer elements.

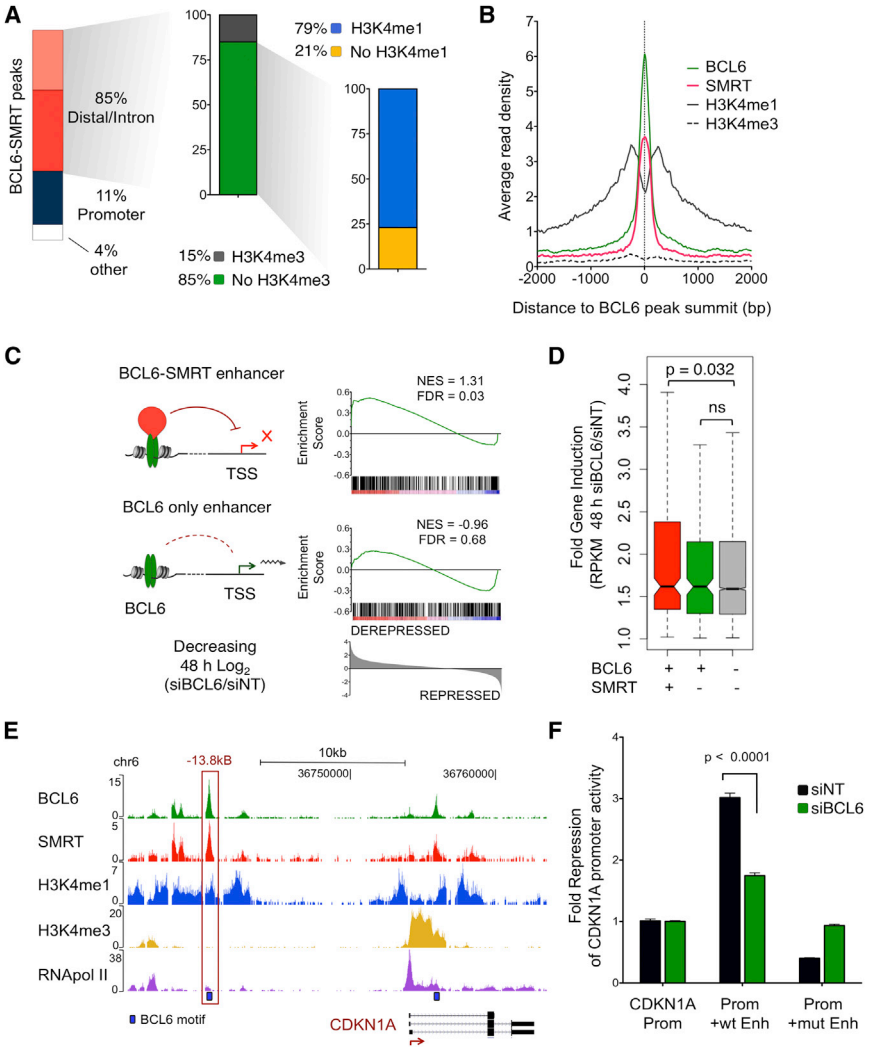

Figure 4. BCL6-SMRT Complexes Mediate Enhancer Silencing

(A) Overlap of distal/intronic BCL6-SMRT peaks with H3K4me3 and H3K4me1 peaks in DLBCL cells.

(B) BCL6, SMRT, and H3K4me1,3 ChIP-seq read density profiles in BCL6-SMRT enhancers centered at the BCL6 peak summit. y axis represents average read densities normalized to total number of reads.

(C) GSEA analysis of genes proximal to BCL6-SMRT-bound enhancers or BCL6 non-SMRT enhancers. Genes were ranked based on decreasing $\log_2$ RPKM (siBCL6/siNT) at 48 hr BCL6 knockdown (weighted p2 statistic, 5,000 permutations).

(D) Comparison of fold expression induction (siBCL6/siNT RPKM, 48 hr) of genes proximal to BCL6-SMRT enhancers or BCL6 non-SMRT enhancers versus other genes.

(E) A BCL6-SMRT enhancer located −13 kb upstream of *CDKN1A* is illustrated. UCSC tracks of BCL6, SMRT, H3K4me1,3, and total RNA polymerase II density normalized to the total number of reads are represented. Location of BCL6 sequence motifs is indicated.

(F) Reporter assays performed in DLBCL cells with constructs containing *CDKN1A* promoter alone (Prom), promoter and wild-type −13 kb enhancer (Prom + WT Enh), or promoter and mutant enhancer (Prom+ mut Enh). Cells were treated with siBCL6 and siNT as indicated in quadruplicates. y axis represents fold repression of reporter based on relative luciferase (versus TK-Renlla) compared to the basal activity of the promoter construct. Data are represented as mean ±SEM. See also Figure S8.

BCL6 Recruitment of SMRT Deacetylates H3K27 to Repress Enhancers

Active enhancers can be distinguished from inactive or "poised" enhancers based on the presence of H3K27 acetylation (Creyghton et al., 2010; Rada-Iglesias et al., 2011). We performed H3K27ac ChIP-seq in DLCBL cells and observed that also in these cells, enhancers with high levels of H3K27ac are associated with highly expressed genes whereas enhancers with low H3K27ac level are associated with lower gene expression ($p < 0.0001$, Mann-Whitney U; Figure S9A). Given the role of H3K27ac in enhancer activation, we hypothesized that BCL6-mediated recruitment of SMRT complex (which contains HDAC3) might deacetylate H3K27, thus rendering these enhancers inactive. Quantitative ChIP assays were performed to detect H3K27ac at BCL6-SMRT enhancers, BCL6-only enhancers, or control loci in DLBCL cells transfected with either BCL6 or control siRNA. BCL6 knockdown increased the relative abundance of H3K27ac at most BCL6-SMRT enhancers but not at BCL6-only enhancers or control loci (Figure 5A). Accompanying the increase in H3K27 acetylation, BCL6 siRNA resulted in a reduction of SMRT recruitment to BCL6-SMRT enhancers (Figure S9B), which paralleled the reduction in BCL6 enrichment (Figure S9C).

Because SMRT complexes contain HDAC3, we hypothesized that this histone deacetylase mediates H3K27 deacetylation. We therefore performed an in vitro HDAC assay using immunoprecipitated SMRT and HDAC3 complexes from DLBCL protein extract incubated with bulk histones, followed by immunoblotting for H3K27ac. This procedure yielded a marked decrease in H3K27ac among histones incubated with SMRT or HDAC3 complexes but not in IgG control pull-downs (Figure 5B). H3K27 deacetylation was abrogated by addition of the HDAC inhibitor Trichostatin A (Figure 5B). To further explore the impact of HDAC3 on H3K27 acetylation in B cells, we isolated splenic B cells from mice with conditional B-lineage-specific deletion of *Hdac3* versus littermate controls. We confirmed reduction of Hdac3 in conditionally deleted B cells by western blotting and observed a reciprocal global increase of the H3K27ac compared to B cells from control mice (Figure 5C).

To test whether disruption of the BCL6-SMRT complex could toggle enhancers to an active state, we treated DLBCL cells with the BCL6 small molecule inhibitor 79-6[1085], which blocks recruitment of corepressors to the BTB domain (Cerchietti

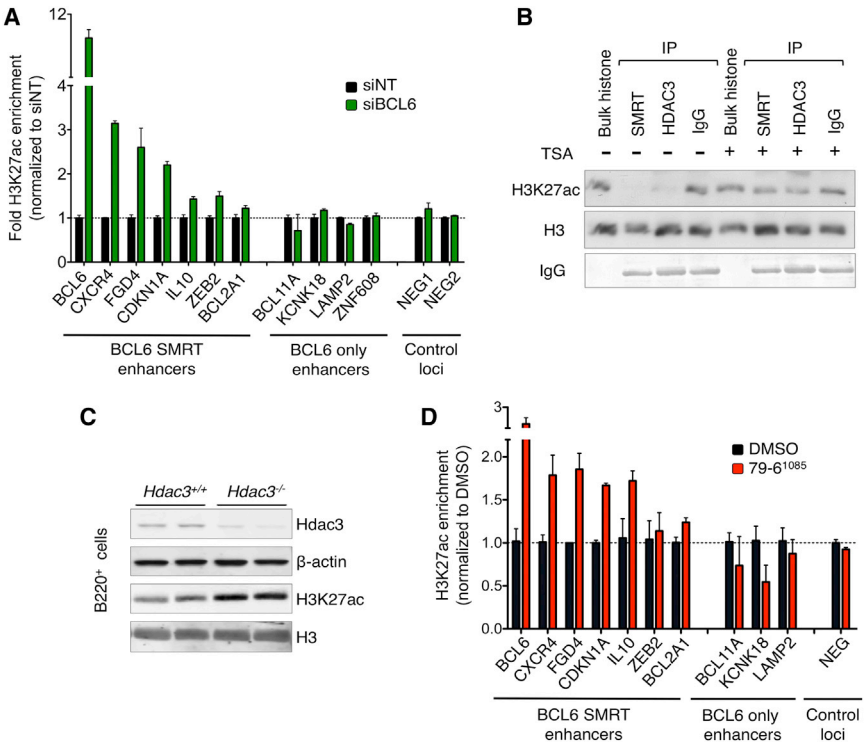

Figure 5. BCL6 Recruits SMRT to Deacetylate H3K27, Leading to Enhancer Inactivation

(A) Selected BCL6-SMRT bound enhancers or BCL6 only enhancers were tested for enrichment of H3K27ac by quantitative ChIP (qChIP) in OCI-Ly1 cells nucleofected with siBCL6 or siNT. Relative enrichment is normalized to siNT and shown as mean ±SEM.

(B) H3K27ac immunoblot of in vitro histone deacetylation reactions using immunoprecipitated SMRT and HDAC3 in the presence or absence of TSA (Trichostatin A). IgG was used as a negative immunoprecipitation control and H3 as a loading control. Coomassie stain indicates that equal amount of antibody was added in each immunoprecipitate.

(C) H3K27ac immunoblot using whole cell extracts of B220+ cells isolated from two Hdac3$^{+/+}$/ROSA-GFP/CD19-Cre and two Hdac3$^{FL/-}$/ROSA-GFP/CD19-Cre mice. Hdac3 depletion in null cells was confirmed. H3 and β-globin were used as loading controls.

(D) Biological replicates of H3K27ac qChIP performed in triplicates in OCI-Ly1 cells exposed to 50 μM of 79-6^{1085} or vehicle (DMSO) for 30 min. Fold H3K27ac enrichment versus vehicle is shown (y axis). Data are represented as mean ± SEM. See also Figure S9.

et al., 2010a). 79-6^{1085} caused the induction of H3K27ac at BCL6-SMRT enhancers but not at enhancers bound by BCL6 alone (Figure 5D). These effects are not due to loss of BCOR since BCOR complex did not deacetylate H3K27 (Figure S9D), nor did BCOR siRNA knockdown induce H3K27 acetylation levels at BCL6 target enhancers Figures S9E and S9F). Collectively, these data suggest that BCL6 recruitment of SMRT results in HDAC3-dependent H3K27 deacetylation of enhancers and gene silencing. By disrupting BCL6 corepressor complexes, BCL6 inhibitors can reactivate the BCL6-repressed enhancer network.

SMRT Corepressor Complexes Antagonize p300 Enhancer Acetylation and Activation

The p300 histone acetyltransferase (HAT) mediates H3K27 acetylation and enhancer activation (Jin et al., 2011; Visel et al., 2009). We hypothesized that BCL6-SMRT complexes would antagonize enhancer activation by p300. We performed p300 ChIP-seq in DLBCL cells and identified a total of 988 p300-bound enhancers. A total of 87% (856/988) of these enhancers were H3K27ac^{HIGH}. We identified 369 enhancers with BCL6-SMRT only, 449 with BCL6-SMRT and p300, and 250 with BCL6-p300, raising the possibility that p300 and SMRT might compete for control of certain BCL6 target enhancers. Indeed, we observed significantly lower levels of H3K27ac in BCL6-SMRT enhancers without p300 ($p < 0.0001$, Mann-Whitney U) and significantly higher levels of H3K27ac in enhancers with BCL6 and p300 but without SMRT ($p < 0.0001$) compared to enhancers that were occupied by BCL6 with both SMRT and p300 (Figure 6A).

In order to more globally evaluate the equilibrium between BCL6-SMRT complex and p300 on H3K27ac levels, we performed H3K27ac ChIP-seq in cells treated with BCL6 or control siRNA (Figure S10A). Consistent with a role for SMRT in antagonizing p300-mediated H3K27ac, BCL6-SMRT enhancers without p300 displayed a greater increase in H3K27ac ($p < 0.0001$, Mann Whitney U) compared to BCL6-SMRT enhancers that also contained p300 (Figure 6B). Moreover, BCL6-SMRT-p300 enhancers in turn featured greater induction of H3K27ac than BCL6 enhancers with p300 but without SMRT ($p < 0.0001$). The greater increase of H3K27ac levels, especially in BCL6-SMRT enhancers, suggests that upon loss of BCL6-SMRT binding, p300 complexes can more efficiently acetylate H3K27.

As a complementary and unbiased approach to determine the link between gene expression and enhancer BCL6 complexes, we performed a multidimensional PCA of distal enhancer BCL6 peaks. Genes associated with one principal component (PC3, n = 715 genes) were notably derepressed upon BCL6 siRNA ($p < 1 \times 10^{-8}$, t test). Consistent with the above data, PC3 featured strong enrichment of BCL6, SMRT, and H3K4me1 but no enrichment for H3K27ac or p300 (Figure 6C). In contrast, PC1 and PC2 genes contained enhancer BCL6 complexes plus p300 with or without enhancer marks, respectively, and were not strongly associated with genes repressed by BCL6. We repeated these analyses on the intronic BCL6-SMRT enhancers (n = 1,344) and observed a comparable association of BCL6-SMRT intronic enhancers with gene derepression, p300 binding, and H3K27ac levels (Figures S10B–S10E). These data were validated using independent BCL6 siRNA

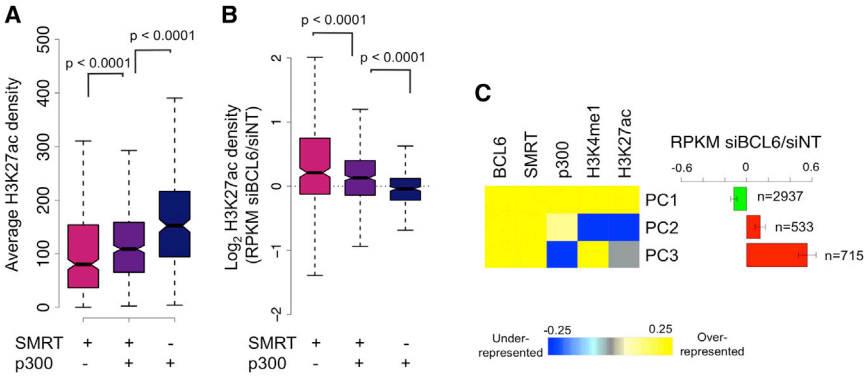

Figure 6. BCL6-SMRT Complexes Antagonize p300 Acetyltransferase Activity to Mediate Enhancer Toggling

(A) Comparison of the average normalized H3K27ac read density levels in BCL6 enhancers bound by SMRT but not p300, bound by both SMRT and p300 or bound by p300 but not SMRT. (B) Log_2 change of H3K27ac levels upon BCL6 knockdown in BCL6 enhancers bound by SMRT but not p300, bound by both SMRT and p300 or bound by p300 but not SMRT. p values are indicated.

(C) Graphical representation of weighted PCA analysis using distal BCL6 binding sites. Correlation with gene expression changes after BCL6 depletion (24 hr) links PC3 (715 distal enhancers, $p < 1 \times 10^{-8}$) to gene derepression. The color key indicates the weights of the original variables assayed by ChIP-seq.

See also Figures S10, S11, S12, S13, and S14.

knockdown RNA-seq replicates as well as additional enhancer histone mark ChIP-seq data sets including H3K4me2, which also marks enhancer regions (Ernst et al., 2011) (Figures S11 and S12). These results suggest that BCL6 recruitment of SMRT/HDAC3 complexes to distal and intronic enhancer regions represses gene expression by deacetylating H3K27ac and opposing the actions of p300 HAT complexes.

Altogether, the data suggest that BCL6 mediates its key biological effects in B cells through at least two biochemically distinct BTB domain-dependent transcriptional repression mechanisms, repressing promoters most potently through multifunctional ternary complexes containing BCOR and SMRT and repressing enhancers through SMRT-HDAC3 actions on H3K27ac (Figure 7). Both of these functions can be therapeutically targeted by BCL6 BTB domain peptide and small molecule inhibitors to kill DLBCL cells or suppress GC formation. Indeed exposure of DLBCL cells to RI-BPI resulted in the same preferential derepression of BCL6 ternary complex promoters and BCL6-SMRT enhancer-associated genes, as observed with BCL6 siRNA (Figure S13).

DISCUSSION

Herein, we report a unique mechanism through which a single transcription factor can serve as scaffold for recruiting structurally and functionally distinct chromatin-modifying complexes through binding to identical surface motifs. We show that BCL6 simultaneously recruits both BCOR and SMRT/NCOR corepressors to symmetrical lateral grooves to form a ternary core repressor complex with BCL6 BTB domain homodimers, yet SMRT and BCOR differ in their disposition around BCL6-regulated promoters. SMRT localizes focally with BCL6 at nucleosome-free regions, whereas BCOR tends to spread downstream of the transcription start site. BCOR downstream spreading may be linked to our observation that BCL6 suppresses RNA Pol II elongation more than preventing loading of Pol II complexes. Repression through promoter ternary complexes is functionally linked to specific epigenetic chromatin marks associated with corepressor enzymatic activities (Gearhart et al., 2006; You et al., 2013).

At enhancers, BCL6-SMRT complexes mediate silencing through a mechanism involving HDAC3 deacetylation of H3K27. SMRT recruitment appears to compete with enhancer activation mediated by p300 through H3K27 acetylation, thus providing a basis for dynamic and reversible "toggling" of enhancers. This would be different from the effect of the histone demethylase LSD1, which permanently erases enhancers through H3K4 demethylation (Whyte et al., 2012). Nonetheless, it remains to be investigated how H3K27 acetylation is linked to enhancer activity. Enhancer toggling may play a physiological role in enabling recycling of B cells between the dark zone and light zone of GCs. Transient interactions with T cells in the light zone triggers CD40 and mitogen-activated protein kinase (MAPK) signaling in B cells, which phosphorylates and delocalizes SMRT and NCOR to the cytoplasm, leading to reversible derepression of BCL6 targets (Polo et al., 2008; Ranuncolo et al., 2007). Presumably, CD40 toggling of BCL6 enhancers enables B cells to become competent for terminal differentiation if they have generated a high-affinity immunoglobulin or to undergo apoptosis if they are damaged or unable to form high-affinity antibody. Toggling back to the repressed state permits recycling of B cells to the dark zone for additional rounds of affinity maturation. Along these lines, it was shown that once CD40 signaling is disengaged, SMRT returns to BCL6 and BCL6 target gene repression is restored (Polo et al., 2008). In support of this notion, analysis of genes that are upregulated in GC light zone B cells (centrocytes) as compared to dark zone cells (centroblasts) (Caron et al., 2009) show significant upregulation of GC B cell BCL6-SMRT enhancer-related target genes but not BCL6-only enhancer genes ($p < 0.0001$, Mann Whitney U; Figures S14A and S14B). BCL6-SMRT enhancer targets were also significantly enriched among centrocyte-upregulated genes (FDR = 0.006, GSEA). Moreover, CD40 signaling and MAPK pathways are strongly enriched among genes regulated by BCL6-SMRT enhancer complexes (Figure S14C).

Enhancer toggling may be pathologically suppressed in certain DLBCLs containing *EP300*-inactivating mutations (Cerchietti et al., 2010b; Pasqualucci et al., 2011). Reduction in EP300 function could tip the balance of transcriptional repression in favor of BCL6-SMRT complexes and thus favor the

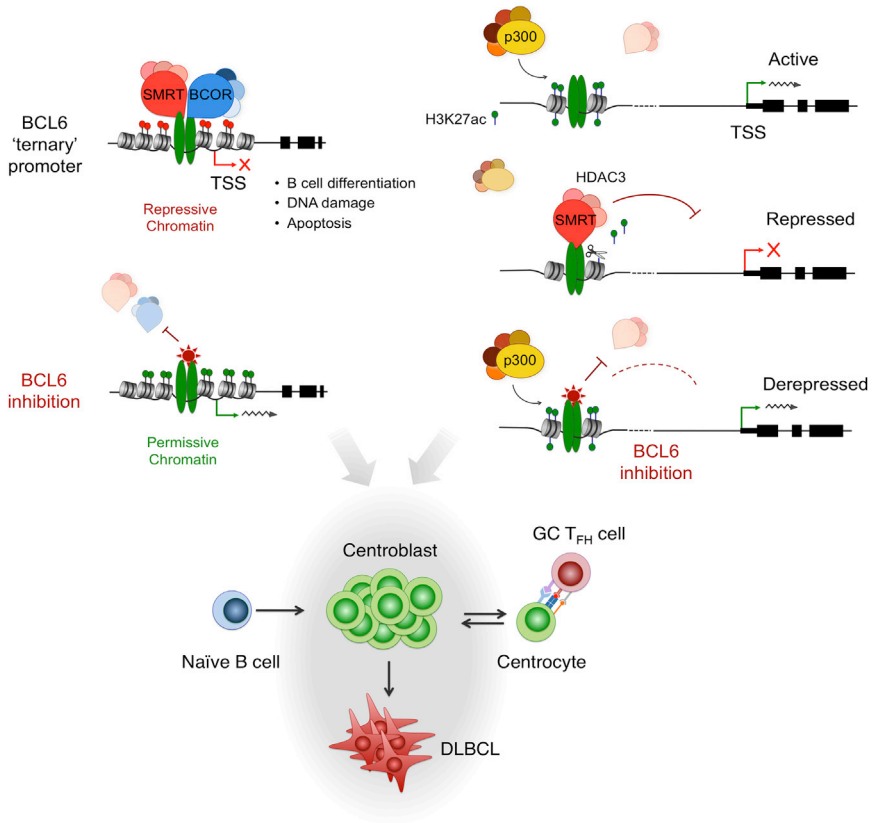

Figure 7. Model of the BCL6 Repression Mechanism

BCL6 dimers can simultaneously recruit PRC1-like BCOR complexes and HDAC3-containing SMRT complexes in B cell promoters to most effectively repress transcription in a repressed chromatin environment. Alternatively, BCL6 selectively recruits SMRT to functionally inactivate a network of B cell enhancers through H3K27 deacetylation, opposing the effect of p300 complexes that mediate H3K27 acetylation. BCL6 BTB inhibitors dismiss BCOR and SMRT complexes and reactivate the BCL6-targeted gene programs, thereby killing lymphoma cells while BCL6-BTB point mutations abrogate GC formation.

oncogenic effects of BCL6. BCL6 BTB blockade was sufficient to induce H3K27ac levels at BCL6-SMRT target enhancers. Hence, enhancer toggling by BCL6 inhibitors may contribute to their antilymphoma effects (Figure 7).

BCL6 ternary complex and BCL6 enhancer complexes seem to be independent of each other, since there was no trend toward overlap at the same genes ($p = 0.957$) and no tendency for the small set of overlapping promoter-enhancer complex-containing genes to be more derepressed after BCL6 siRNA ($p = 0.44$, Mann Whitney test, data not shown). Specific BCL6 target gene sets may thus be independently controlled through its two different BTB-domain-dependent repression mechanisms. Collectively the BTB-dependent mechanisms we identified are essential for DLBCLs and the normal GC B cells from which they are derived (e.g., as in Figures 1A and S3A). However, our data do not rule out that other BCL6 repression mechanisms may exist and contribute in some way to its actions in B cells or other cell types (Mendez et al., 2008; Parekh et al., 2007). Further research into the biochemistry of BCL6 in B cells and other cell types is warranted to explore this question. It is notable that BCL6 was also shown to be localized at enhancers in macrophages (Barish et al., 2012). However, BCL6 functions at macrophage enhancer actions are likely mechanistically different than B cells since BTB-domain-dependent corepressor recruitment is dispensable for the actions of BCL6 in this cell type (Huang et al., 2013).

In summary, our data highlight the flexibility of BCL6 to simultaneously regulate gene expression through different mechanisms on different gene sets within the same cells, through the same protein interface. From the immunology perspective, it is notable that these mechanisms are specifically significant to B cells but may not play a major role in the actions of BCL6 in T cells or macrophages (Huang et al., 2013). Hence, BCL6 displays a tremendous degree of flexibility and complexity in the immune system. Importantly, therapeutic targeting of BCL6 with inhibitors that block the BTB lateral groove results in simultaneous blockade of both BTB-dependent mechanisms but has no effect on other compartments of the immune system. This enables cell-type-specific inhibition of BCL6 in lymphomas and B cells without needing to resort to complicated tissue-specific delivery systems. Finally, although our current studies have focused on BCL6, it is likely that enhancer toggling and biochemical functional diversity are more general mechanisms relevant to other enhancer transcription factors.

EXPERIMENTAL PROCEDURES

All procedures involving animals were approved by the Animal Institute Committee at the Weill Cornell Medical College of Cornell University.

Chromatin Immunoprecipitation

OCI-Ly1 or purified GC B cells were fixed, lysed, and sonicated to generate fragments less than 400 bp. Sonicated lysates were incubated with antibodies overnight (see Extended Experimental Procedures), and after increasing stringency washes immunocomplexes were recovered and DNA was isolated. ChIP and input DNA was used in qPCR reactions to estimate relative enrichment. In experiments using drug treatments (Figure 5D), cells were treated with compounds (50 μM) for 30 min and after completion of the assay ChIP and input DNA was quantified using Qubit 2.0 fluorometer (Invitrogen) so that an equal amount of DNA was added to each PCR reaction.

Details regarding the antibodies and primers used in this study can be found in the Extended Experimental Procedures and in Tables S2, S3, and S4.

ChIP-re-ChIP

Experiments were performed as above. After the first round of ChIP, immunocomplexes were eluted by incubating the beads in 50 μl TE buffer

supplemented with 10 mM DTT and protease inhibitors for 30 min at 37°C rocking. The eluted immunocomplexes were diluted up to 1 ml with dilution buffer (1% Triton X-100, 2 mM EDTA, 20 mM Tris-HCl [pH 8.1], 150 mM NaCl, and protease inhibitors) and antibodies were added for a second round of ChIP. Finally, the bound DNA was eluted and enrichment was quantified by qPCR of PCR products.

ChIP-Seq

ChIP-seq libraries were prepared using the Illumina ChIP-seq Library preparation kit following the manufacturer's instructions with minor modifications starting with 10 ng of purified ChIP DNA (see Extended Experimental Procedures). An input chromatin control library was generated for each ChIP-seq experiment starting from the same amount of material and was used as a negative control for peak calling and downstream analyses using the ChIPseeqer package (Giannopoulou and Elemento, 2011). Details on Illumina data analysis can be found in the Extended Experimental Procedures.

Gene Expression Analysis by mRNA-Seq

A total of 3 μg of total RNA was isolated from at 24 hr and 48 hr after siRNA nucleofection. The RNAeasy Plus Kit (QIAGEN) that included a genomic DNA elimination step was used for RNA isolation. RNA concentration and purity were determined using Nanodrop (Thermo Scientific) and integrity was verified using Agilent 2100 Bioanalyzer (Agilent Technologies). Libraries were generated using an mRNA-seq sample prep kit (Illumina). Briefly, mRNA was selected by two rounds of purification using magnetic polydT beads and then fragmented. First-strand synthesis was performed using random oligos and SuperscriptIII (Invitrogen). After second-strand synthesis, a 200 bp paired-end library was prepared following the Illumina paired-end library preparation protocol.

Statistical Analysis

The two-tailed Mann-Whitney U test was used unless otherwise stated. For details on PCA analysis, see the Extended Experimental Procedures. All statistical analyses were carried out using Prism software (Graphpad) and the R statistical package.

ACCESSION NUMBERS

The Gene Expression Omnibus (GEO) accession number for the ChIP-seq and RNA-seq data sets reported in this paper is GSE29282. Additional ChIP-seq data were analyzed that we previously reported under accession number GSE43350.

SUPPLEMENTAL INFORMATION

Supplemental Information includes Extended Experimental Procedures, fourteen figures, and four tables and can be found with this article online at http://dx.doi.org/10.1016/j.celrep.2013.06.016.

ACKNOWLEDGMENTS

We would like to thank the members of the Melnick lab for their support and constructive discussions, Grant Barish and Ron Evans for providing the NCOR antibody used in this study, Mariano Cardenas and Connie Marie Corcoran for technical assistance, and the Weill Cornell Epigenomics Core for high-throughput data processing. This work was supported by NCI R01 CA104348 (A.M.), NCI R01 CA071540 (V.B.), and NSF CAREER grant 1054964 (O.E.). A.M. is supported by the Chemotherapy Foundation and the Burroughs Wellcome Foundation. F.G.B. is supported by a Sass Foundation Judah Folkman Fellowship. L.C. is a Raymond and Beverly Sackler Scholar. J.M.P. is supported by the NHMRC and Monash Larkins Program. G.G.P. and K.K. were funded by the CCSRI. This research was also made possible by the Raymond and Beverly Sackler Center for Biomedical and Physical Sciences at Weill Cornell Medical College.

Received: March 7, 2013
Revised: May 13, 2013
Accepted: June 11, 2013
Published: August 1, 2013

REFERENCES

Ahmad, K.F., Melnick, A., Lax, S., Bouchard, D., Liu, J., Kiang, C.L., Mayer, S., Takahashi, S., Licht, J.D., and Privé, G.G. (2003). Mechanism of SMRT corepressor recruitment by the BCL6 BTB domain. Mol. Cell *12*, 1551–1564.

Barish, G.D., Yu, R.T., Karunasiri, M.S., Becerra, D., Kim, J., Tseng, T.W., Tai, L.J., Leblanc, M., Diehl, C., Cerchietti, L., et al. (2012). The Bcl6-SMRT/NCoR cistrome represses inflammation to attenuate atherosclerosis. Cell Metab. *15*, 554–562.

Basso, K., Klein, U., Niu, H., Stolovitzky, G.A., Tu, Y., Califano, A., Cattoretti, G., and Dalla-Favera, R. (2004). Tracking CD40 signaling during germinal center development. Blood *104*, 4088–4096.

Caron, G., Le Gallou, S., Lamy, T., Tarte, K., and Fest, T. (2009). CXCR4 expression functionally discriminates centroblasts versus centrocytes within human germinal center B cells. J. Immunol. *182*, 7595–7602.

Cerchietti, L.C., Yang, S.N., Shaknovich, R., Hatzi, K., Polo, J.M., Chadburn, A., Dowdy, S.F., and Melnick, A. (2009). A peptomimetic inhibitor of BCL6 with potent antilymphoma effects in vitro and in vivo. Blood *113*, 3397–3405.

Cerchietti, L.C., Ghetu, A.F., Zhu, X., Da Silva, G.F., Zhong, S., Matthews, M., Bunting, K.L., Polo, J.M., Farès, C., Arrowsmith, C.H., et al. (2010a). A small-molecule inhibitor of BCL6 kills DLBCL cells in vitro and in vivo. Cancer Cell *17*, 400–411.

Cerchietti, L.C., Hatzi, K., Caldas-Lopes, E., Yang, S.N., Figueroa, M.E., Morin, R.D., Hirst, M., Mendez, L., Shaknovich, R., Cole, P.A., et al. (2010b). BCL6 repression of EP300 in human diffuse large B cell lymphoma cells provides a basis for rational combinatorial therapy. J. Clin. Invest. *120*, 4569–4582.

Ci, W., Polo, J.M., and Melnick, A. (2008). B-cell lymphoma 6 and the molecular pathogenesis of diffuse large B-cell lymphoma. Curr. Opin. Hematol. *15*, 381–390.

Ci, W., Polo, J.M., Cerchietti, L., Shaknovich, R., Wang, L., Yang, S.N., Ye, K., Farinha, P., Horsman, D.E., Gascoyne, R.D., et al. (2009). The BCL6 transcriptional program features repression of multiple oncogenes in primary B cells and is deregulated in DLBCL. Blood *113*, 5536–5548.

Creyghton, M.P., Cheng, A.W., Welstead, G.G., Kooistra, T., Carey, B.W., Steine, E.J., Hanna, J., Lodato, M.A., Frampton, G.M., Sharp, P.A., et al. (2010). Histone H3K27ac separates active from poised enhancers and predicts developmental state. Proc. Natl. Acad. Sci. USA *107*, 21931–21936.

Dent, A.L., Shaffer, A.L., Yu, X., Allman, D., and Staudt, L.M. (1997). Control of inflammation, cytokine expression, and germinal center formation by BCL-6. Science *276*, 589–592.

Ernst, J., Kheradpour, P., Mikkelsen, T.S., Shoresh, N., Ward, L.D., Epstein, C.B., Zhang, X., Wang, L., Issner, R., Coyne, M., et al. (2011). Mapping and analysis of chromatin state dynamics in nine human cell types. Nature *473*, 43–49.

Farcas, A.M., Blackledge, N.P., Sudbery, I., Long, H.K., McGouran, J.F., Rose, N.R., Lee, S., Sims, D., Cerase, A., Sheahan, T.W., et al. (2012). KDM2B links the Polycomb Repressive Complex 1 (PRC1) to recognition of CpG islands. Elife *1*, e00205.

Gao, Z., Zhang, J., Bonasio, R., Strino, F., Sawai, A., Parisi, F., Kluger, Y., and Reinberg, D. (2012). PCGF homologs, CBX proteins, and RYBP define functionally distinct PRC1 family complexes. Mol. Cell *45*, 344–356.

Gearhart, M.D., Corcoran, C.M., Wamstad, J.A., and Bardwell, V.J. (2006). Polycomb group and SCF ubiquitin ligases are found in a novel BCOR complex that is recruited to BCL6 targets. Mol. Cell. Biol. *26*, 6880–6889.

Ghetu, A.F., Corcoran, C.M., Cerchietti, L., Bardwell, V.J., Melnick, A., and Privé, G.G. (2008). Structure of a BCOR corepressor peptide in complex with the BCL6 BTB domain dimer. Mol. Cell *29*, 384–391.

Giannopoulou, E.G., and Elemento, O. (2011). An integrated ChIP-seq analysis platform with customizable workflows. BMC Bioinformatics *12*, 277.

Heintzman, N.D., Stuart, R.K., Hon, G., Fu, Y., Ching, C.W., Hawkins, R.D., Barrera, L.O., Van Calcar, S., Qu, C., Ching, K.A., et al. (2007). Distinct and predictive chromatin signatures of transcriptional promoters and enhancers in the human genome. Nat. Genet. *39*, 311–318.

Heintzman, N.D., Hon, G.C., Hawkins, R.D., Kheradpour, P., Stark, A., Harp, L.F., Ye, Z., Lee, L.K., Stuart, R.K., Ching, C.W., et al. (2009). Histone modifications at human enhancers reflect global cell-type-specific gene expression. Nature *459*, 108–112.

Huang, C., Hatzi, K., and Melnick, A. (2013). Lineage-specific functions of BCL6 in immunity and inflammation are mediated through distinct biochemical mechanisms. Nat. Immunol. *14*, 380–388.

Jin, Q., Yu, L.R., Wang, L., Zhang, Z., Kasper, L.H., Lee, J.E., Wang, C., Brindle, P.K., Dent, S.Y., and Ge, K. (2011). Distinct roles of GCN5/PCAF-mediated H3K9ac and CBP/p300-mediated H3K18/27ac in nuclear receptor transactivation. EMBO J. *30*, 249–262.

Karagianni, P., and Wong, J. (2007). HDAC3: taking the SMRT-N-CoRrect road to repression. Oncogene *26*, 5439–5449.

Lam, L.T., Wright, G., Davis, R.E., Lenz, G., Farinha, P., Dang, L., Chan, J.W., Rosenwald, A., Gascoyne, R.D., and Staudt, L.M. (2008). Cooperative signaling through the signal transducer and activator of transcription 3 and nuclear factor-kappaB pathways in subtypes of diffuse large B-cell lymphoma. Blood *111*, 3701–3713.

Mendez, L.M., Polo, J.M., Yu, J.J., Krupski, M., Ding, B.B., Melnick, A., and Ye, B.H. (2008). CtBP is an essential corepressor for BCL6 autoregulation. Mol. Cell. Biol. *28*, 2175–2186.

Parekh, S., Polo, J.M., Shaknovich, R., Juszczynski, P., Lev, P., Ranuncolo, S.M., Yin, Y., Klein, U., Cattoretti, G., Dalla Favera, R., et al. (2007). BCL6 programs lymphoma cells for survival and differentiation through distinct biochemical mechanisms. Blood *110*, 2067–2074.

Parekh, S., Privé, G., and Melnick, A. (2008). Therapeutic targeting of the BCL6 oncogene for diffuse large B-cell lymphomas. Leuk. Lymphoma *49*, 874–882.

Pasqualucci, L., Dominguez-Sola, D., Chiarenza, A., Fabbri, G., Grunn, A., Trifonov, V., Kasper, L.H., Lerach, S., Tang, H., Ma, J., et al. (2011). Inactivating mutations of acetyltransferase genes in B-cell lymphoma. Nature *471*, 189–195.

Perissi, V., Jepsen, K., Glass, C.K., and Rosenfeld, M.G. (2010). Deconstructing repression: evolving models of co-repressor action. Nat. Rev. Genet. *11*, 109–123.

Phan, R.T., and Dalla-Favera, R. (2004). The BCL6 proto-oncogene suppresses p53 expression in germinal-centre B cells. Nature *432*, 635–639.

Polo, J.M., Dell'Oso, T., Ranuncolo, S.M., Cerchietti, L., Beck, D., Da Silva, G.F., Prive, G.G., Licht, J.D., and Melnick, A. (2004). Specific peptide interference reveals BCL6 transcriptional and oncogenic mechanisms in B-cell lymphoma cells. Nat. Med. *10*, 1329–1335.

Polo, J.M., Ci, W., Licht, J.D., and Melnick, A. (2008). Reversible disruption of BCL6 repression complexes by CD40 signaling in normal and malignant B cells. Blood *112*, 644–651.

Rada-Iglesias, A., Bajpai, R., Swigut, T., Brugmann, S.A., Flynn, R.A., and Wysocka, J. (2011). A unique chromatin signature uncovers early developmental enhancers in humans. Nature *470*, 279–283.

Ranuncolo, S.M., Polo, J.M., Dierov, J., Singer, M., Kuo, T., Greally, J., Green, R., Carroll, M., and Melnick, A. (2007). Bcl-6 mediates the germinal center B cell phenotype and lymphomagenesis through transcriptional repression of the DNA-damage sensor ATR. Nat. Immunol. *8*, 705–714.

Saito, M., Novak, U., Piovan, E., Basso, K., Sumazin, P., Schneider, C., Crespo, M., Shen, Q., Bhagat, G., Califano, A., et al. (2009). BCL6 suppression of BCL2 via Miz1 and its disruption in diffuse large B cell lymphoma. Proc. Natl. Acad. Sci. USA *106*, 11294–11299.

Sánchez, C., Sánchez, I., Demmers, J.A., Rodriguez, P., Strouboulis, J., and Vidal, M. (2007). Proteomics analysis of Ring1B/Rnf2 interactors identifies a novel complex with the Fbxl10/Jhdm1B histone demethylase and the Bcl6 interacting corepressor. Mol. Cell. Proteomics *6*, 820–834.

Shaffer, A.L., Yu, X., He, Y., Boldrick, J., Chan, E.P., and Staudt, L.M. (2000). BCL-6 represses genes that function in lymphocyte differentiation, inflammation, and cell cycle control. Immunity *13*, 199–212.

Stogios, P.J., Downs, G.S., Jauhal, J.J., Nandra, S.K., and Privé, G.G. (2005). Sequence and structural analysis of BTB domain proteins. Genome Biol. *6*, R82.

Visel, A., Blow, M.J., Li, Z., Zhang, T., Akiyama, J.A., Holt, A., Plajzer-Frick, I., Shoukry, M., Wright, C., Chen, F., et al. (2009). ChIP-seq accurately predicts tissue-specific activity of enhancers. Nature *457*, 854–858.

Wang, X., Li, Z., Naganuma, A., and Ye, B.H. (2002). Negative autoregulation of BCL-6 is bypassed by genetic alterations in diffuse large B cell lymphomas. Proc. Natl. Acad. Sci. USA *99*, 15018–15023.

Whyte, W.A., Bilodeau, S., Orlando, D.A., Hoke, H.A., Frampton, G.M., Foster, C.T., Cowley, S.M., and Young, R.A. (2012). Enhancer decommissioning by LSD1 during embryonic stem cell differentiation. Nature *482*, 221–225.

You, S.H., Lim, H.W., Sun, Z., Broache, M., Won, K.J., and Lazar, M.A. (2013). Nuclear receptor co-repressors are required for the histone-deacetylase activity of HDAC3 in vivo. Nat. Struct. Mol. Biol. *20*, 182–187.